Geometrical Isomerism of Bis(alkyl trithiocarbonato-*S,S'*)bis-(triphenylphosphine) Complexes of Osmium-(II) and -(III)

Amitava Pramanik, Nilkamal Bag, Goutam Kumar Lahiri and Animesh Chakravorty *
Department of Inorganic Chemistry, Indian Association for the Cultivation of Science, Calcutta 700032, India

Complexes of types $[Os(RSCS_2)_2(PPh_3)_2]^z$ (*cis*-Os^{II}, $z = 0$, **1**; *cis*-Os^{III}, $z = +$, $\mathbf{1}^+$; *trans*-Os^{II}, $z = 0$, **2**; and *trans*-Os^{III}, $z = +$, $\mathbf{2}^+$) have been prepared, but $\mathbf{1}^+$ is observable only in solution. The $\mathbf{2}^+$ salts are paramagnetic ($S = \frac{1}{2}$) and display rhombic EPR spectra which have been analysed; a relatively weak electronic transition observed in NIR region is assigned to excitation from one Kramers doublet to another. Electrochemical and spectral data have been used to characterise the coupled redox and isomerisation processes interlinking **1**, $\mathbf{1}^+$, **2** and $\mathbf{2}^+$. Upon oxidation **1** affords $\mathbf{1}^+$ which isomerises to $\mathbf{2}^+$ relatively rapidly. On the other hand, $\mathbf{2}^+$ can be reduced to **2** which slowly but spontaneously isomerises to **1**. Rate and equilibrium data are reported. The electronic and steric factors controlling isomer preference [*cis* for osmium(II) and *trans* for osmium(III)] are noted. Compared to the present complexes, the ruthenium congeners isomerise more rapidly and more completely.

Different oxidation states of the same metal ion may have distinctly different bonding qualities. For example bivalent ruthenium and osmium are good d_π donors but the trivalent metals are not.[1] Isomeric co-ordination spheres will generally differ in bonding and steric properties. One may therefore expect that unequal metal oxidation states may be able to differentiate isomeric co-ordination spheres in one way or another. This theme has received attention.[2–6] In a recent communication [7] we have examined the structural basis of such differentiation in the case of the mixed trithiocarbonate–phosphine osmium system $[Os(EtSCS_2)_2(PPh_3)_2]^z$ ($z = 0$ or 1). Herein we present a full report on the synthesis, spectra and electrochemistry of the $[Os(RSCS_2)_2(PPh_3)_2]^z$ (R = Et, Pr^i or $PhCH_2$) family in relation to isomerisation and structure.

Results and Discussion

Synthesis and Characterisation.—The complexes and isomers in this work are of types **1**, $\mathbf{1}^+$, **2** and $\mathbf{2}^+$. All except $\mathbf{1}^+$ have been isolated in the crystalline state. The primary synthetic reaction is that between $[Os(PPh_3)_3Br_2]$ and $K[RSCS_2]$ in ethanol affording **1**. This complex is stoichiometrically oxidised by Ce^{IV} furnishing $\mathbf{2}^+$ which is isolated as its PF_6^- salt. Reduction of $\mathbf{2}^+$ by $N_2H_4 \cdot H_2O$ affords **2**. Yields are excellent for all steps. The complexes isolated are listed in Table 1 along with elemental analyses and electronic spectral data. Representative spectra are shown in Fig. 1. The $[\mathbf{2}]^+[PF_6]^-$ salts behave as 1:1 electrolytes in acetonitrile solution ($\Lambda = 135$–$150\ \Omega^{-1}\ cm^2\ mol^{-1}$). Apart from our earlier report,[7] no trithiocarbonates of osmium have been described. The geometries of **1**, **2** and $\mathbf{2}^+$ are known (R = Et) beyond doubt from X-ray data.[7]

The $[\mathbf{2}]^+[PF_6]^-$ complexes behave as one-electron paramagnets and in dichloromethane–toluene glasses (77 K) they display rhombic EPR spectra (Fig. 2, Table 2). In the crystalline state $[Os(EtSCS_2)_2(PPh_3)_2]^+$ is centrosymmetric but the maximum axial symmetry is only two-fold.[7] The rhombic nature of the EPR spectrum is therefore expected. The spectra have been analysed in terms of the *g*-tensor theory of low-spin d^5 ions (t_2^5).[8,9] Axial (Δ) and rhombic (V) distortion combined with spin–orbit coupling [λ; for Os^{III} λ is 3000 cm^{-1} (ref. 10)] transform the t_2 shell into three Kramers doublets. The ligand-field transitions (ν_1 and ν_2) among them are predicted to lie at ≈ 7200 and 10 000 cm^{-1}. A relatively weak transition is indeed observed near 7500 cm^{-1} (Fig. 2) and is assigned to ν_1 (Table 2). The ν_2 band is not observed probably because it is obscured by the rising tail of the more intense band at ≈ 670 nm (Table 1).

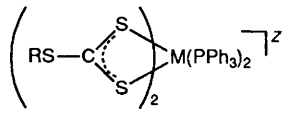

R = Et, Pr^i, or $PhCH_2$

	M	Z	Structure
cis	Os^{II}	0	**1**
cis	Os^{III}	+	$\mathbf{1}^+$
trans	Os^{II}	0	**2**
trans	Os^{III}	+	$\mathbf{2}^+$

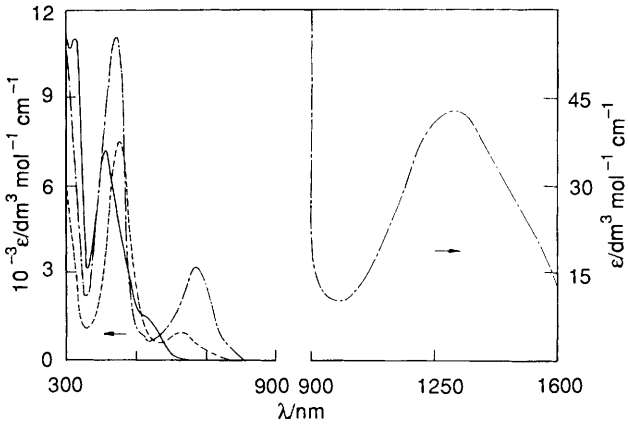

Fig. 1 Electronic spectra of *cis*-$[Os(Pr^iSCS_2)_2(PPh_3)_2]$ (——), *trans*-$[Os(Pr^iSCS_2)_2(PPh_3)_2]$ (– – –) and *trans*-$[Os(Pr^iSCS_2)_2(PPh_3)_2]PF_6$ (–·–·–) in dichloromethane at 298 K

Redox Equilibria and Isomerisation.—Voltammetric and spectral studies have disclosed the occurrence of geometrical isomerisation following electron transfer at the metal. The results can be rationalised in terms of the cycle shown in

Table 1 Analytical and electronic spectral data[a]

Compound	Analysis (%)[b] C	H	UV/VIS and NIR spectral data, λ_{max}/nm (ε/dm^3 mol^{-1} cm^{-1})
cis-[Os(EtSCS$_2$)$_2$(PPh$_3$)$_2$]	51.25 (51.00)	4.15 (4.05)	520(sh)(1890), 420(8660), 320(12 750), 270(sh)(23 030)
cis-[Os(Pr^{i}SCS$_2$)$_2$(PPh$_3$)$_2$]	52.15 (51.95)	4.50 (4.35)	525(sh)(1500), 415(7250), 320(11 080), 270(sh)(19 720)
cis-[Os(PhCH$_2$SCS$_2$)$_2$(PPh$_3$)$_2$]	56.40 (56.10)	4.10 (3.95)	520(sh)(1780), 420(8780), 320(12 350), 270(sh)(21 040)
trans-[Os(EtSCS$_2$)$_2$(PPh$_3$)$_2$]	51.10 (51.00)	4.10 (4.05)	640(1070), 450(10 300), 285(16 480)
trans-[Os(Pr^{i}SCS$_2$)$_2$(PPh$_3$)$_2$]	52.05 (51.95)	4.35 (4.35)	635(980), 450(9065), 290(15 140)
trans-[Os(PhCH$_2$SCS$_2$)$_2$(PPh$_3$)$_2$]	56.10 (56.10)	4.05 (3.95)	640(1170), 450(12 400), 285(20 670)
trans-[Os(EtSCS$_2$)$_2$(PPh$_3$)$_2$]PF$_6$	44.50 (44.50)	3.50 (3.55)	1325(43), 670(3210), 510(sh)(960), 440(12 080), 260(26 470)
trans-[Os(Pr^{i}SCS$_2$)$_2$(PPh$_3$)$_2$]PF$_6$	45.50 (45.45)	3.80 (3.80)	1300(43), 665(3190), 515(sh)(880), 440(11 070), 260(26 670)
trans-[Os(PhCH$_2$SCS$_2$)$_2$(PPh$_3$)$_2$]PF$_6$	49.60 (49.65)	3.55 (3.50)	1325(42), 670(3860), 510(sh)(1000), 440(15 340), 260(36 500)

[a] In dichloromethane at 298 K. [b] Calculated values are in parentheses.

Table 2 Magnetic moments,[a] EPR g values,[b] distortion parameters, and NIR transitions[c] for *trans*-[Os(RSCS$_2$)$_2$(PPh$_3$)$_2$]PF$_6$

R	μ_{eff}	g_x	g_y	g_z	Δ/λ	V/λ	ν_1/λ	ν_2/λ	ν_1/λ (Obs[d])
Et	1.87	2.751	2.552	1.447	2.529	−0.539	2.398	3.332	2.516
Pr^i	1.90	2.762	2.543	1.448	2.539	−0.596	2.391	3.357	2.564
PhCH$_2$	1.76	2.739	2.582	1.485	2.634	−0.454	2.505	3.405	2.516

[a] In the solid state at 298 K. [b] Measurements were made in dichloromethane–toluene (1:1) glass at 77 K. [c] Symbols have the same meaning as in the text. [d] Observed frequency converted into ν_1/λ by setting λ = 3000 cm^{-1}.

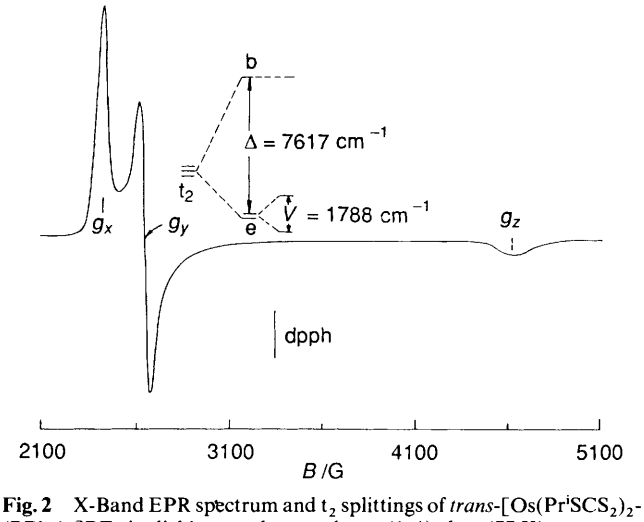

Fig. 2 X-Band EPR spectrum and t_2 splittings of *trans*-[Os(Pr^{i}SCS$_2$)$_2$(PPh$_3$)$_2$]PF$_6$ in dichloromethane–toluene (1:1) glass (77 K)

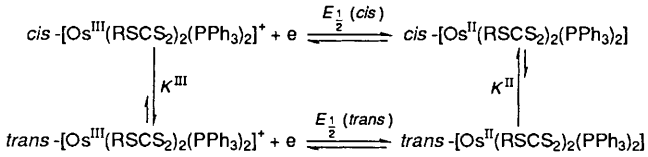

Scheme 1

Scheme 1. Voltammetric experiments were performed in the temperature range 248–308 K in dichloromethane solution at a platinum electrode. Representative voltammograms are shown in Fig. 3 and $E_{\frac{1}{2}}$ data in Table 3. All potentials are referred to the saturated calomel electrode (SCE).

The behaviour of the complexes of type **1** will be considered

Table 3 Electrochemical data*

Compound	$E_{\frac{1}{2}}$(Os^{III}–Os^{II})/V *cis*	*trans*
[Os(EtSCS$_2$)$_2$(PPh$_3$)$_2$]	0.43	0.15
[Os(Pr^{i}SCS$_2$)$_2$(PPh$_3$)$_2$]	0.41	0.15
[Os(PhCH$_2$SCS$_2$)$_2$(PPh$_3$)$_2$]	0.47	0.17

* Conditions: 298 K; solvent, dichloromethane; supporting electrolyte, NEt_4ClO_4 (0.1 mol dm^{-3}); working electrode, platinum; reference electrode, SCE; solute concentration, $\approx 10^{-3}$ mol dm^{-3}. $E_{\frac{1}{2}} = 0.5(E_{p_a} + E_{p_c})$, where E_{p_a} and E_{p_c} are anodic and cathodic cyclic voltammetric peak potentials respectively; scan rate, 50 mV s^{-1}.

first, Fig. 3(*a*). The one-electron (confirmed coulometrically) anodic peak near 0.6 V is assigned to the stereoretentive metal oxidation **1** ⟶ **1**$^+$. Complex **1**$^+$ so formed isomerises rapidly to **2**$^+$ at *e.g.* 298 K and consequently the peak due to reduction of **1**$^+$ is not observed on scan reversal. On the other hand a relatively small cathodic peak is observed near 0.1 V due to the reduction **2**$^+$ ⟶ **2**. In the second and subsequent cycles the oxidation **2** ⟶ **2**$^+$ becomes observable as an anodic peak near 0.2 V. When the solution is cooled the isomerisation **1**$^+$ ⟶ **2**$^+$ is retarded as can be seen from the growth of cathodic peak near 0.4 V due to the reduction **1**$^+$ ⟶ **1**. Thus the *cis* complex **1**$^+$ is observable electrochemically but we have not so far succeeded in isolating it due to its facile conversion into **2**$^+$. We have noted earlier that Ce^{IV} oxidises **1** to **2**$^+$; evidently **1**$^+$ is formed as an intermediate only to isomerise rapidly to **2**$^+$. Similarly, when **1** is coulometrically oxidised at 0.8 V, one electron is quantitatively transferred but the solution is found to contain only **2**$^+$ even when coulometry is performed at 248 K.

At 248 K the voltammogram of complex **2**$^+$, Fig. 3(*b*), corresponds simply to the one-electron couple **2**$^+$/**2**, uncompli-

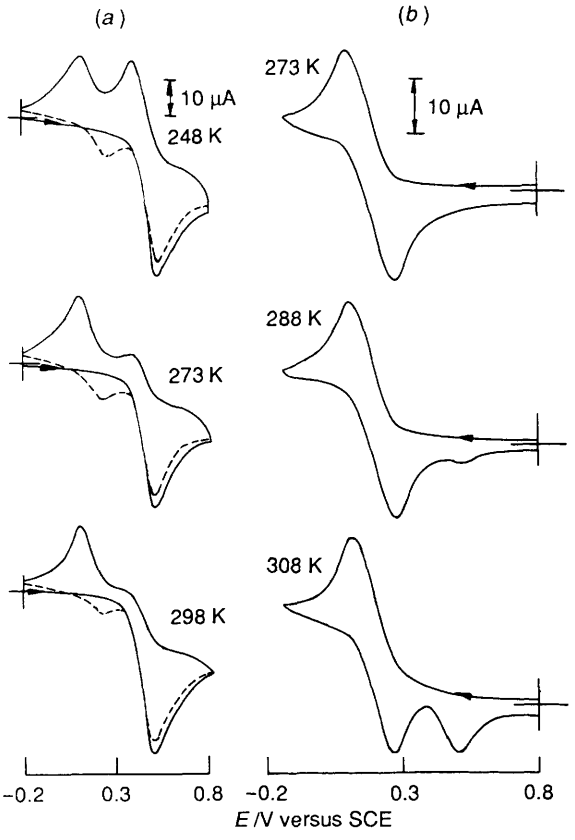

Fig. 3 Variable-temperature cyclic voltammograms (scan rate 50 mV s^{-1}) of $\approx 10^{-3}$ mol dm^{-3} solutions of (*a*) *cis*-$[Os(EtSCS_2)_2(PPh_3)_2]$ [first cycle (——), second cycle (– – –)] and (*b*) *trans*-$[Os(EtSCS_2)_2(PPh_3)_2]PF_6$ in dichloromethane (0.1 mol dm^{-3} $[NEt_4][ClO_4]$) at a platinum electrode

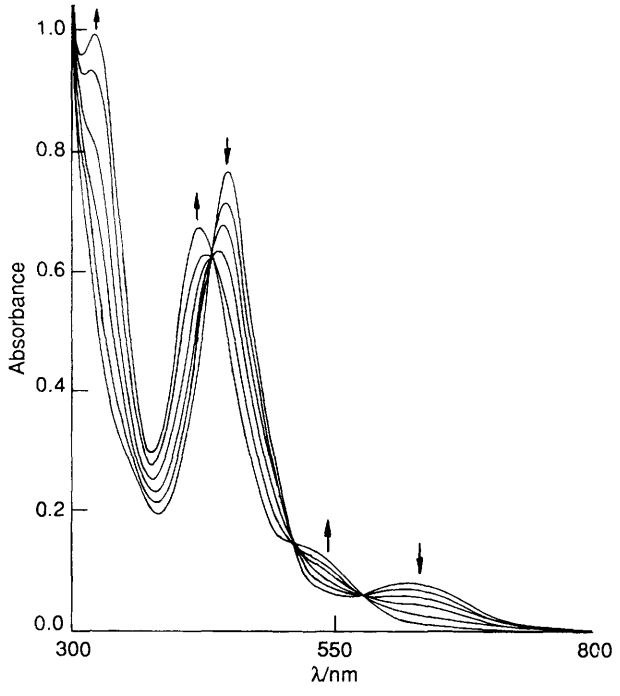

Fig. 4 Time evolution of the electronic spectra of an isomerising solution of *trans*-$[Os(Pr^iSCS_2)_2(PPh_3)_2]$ in dichloromethane at 303 K. The arrows indicate increase and decrease in band intensities as the reaction proceeds

cated by isomerisation. Increasing temperature leads to the onset of the isomerisation process **2** ⟶ **1** as revealed by the appearance of the anodic peak due to the oxidation **1** ⟶ $\mathbf{1}^+$. The higher the temperature the more pronounced is the peak. At a given temperature, the cyclic voltammogram of solutions of **2** (initial scan anodic) is the same as that of $\mathbf{2}^+$ (initial scan cathodic), as expected.

When $\mathbf{2}^+$ is coulometrically reduced (0.0 V) at 248 K **2** is formed quantitatively; the latter reverts back to $\mathbf{2}^+$ upon oxidation at 0.4 V. When the reduction of $\mathbf{2}^+$ is performed at higher temperatures, say 298 K, **2** is again formed but it now isomerises to **1**, though relatively slowly.

The rates of the isomerisation steps (both first order) **2** ⟶ **1** and $\mathbf{1}^+$ ⟶ $\mathbf{2}^+$ have been determined, the former spectrophotometrically and the latter from cyclic voltammetric current heights.[11] The time evolution of the spectrum of a complex of type **2** is shown in Fig. 4. Variable-temperature rate constants and activation parameters are collected in Table 4. The $\mathbf{1}^+$ ⟶ $\mathbf{2}^+$ isomerisation is characterised by a sizeable negative entropy and this is suggestive of a twist mechanism.[12] The same could be true for the **2** ⟶ **1** isomerisation but here bond weakening may be more significant.

We now consider the equilibrium constants K^{II} and K^{III} (Scheme 1) as defined in equations (1) and (2). Complex **2**

$$K^{II} = [\mathbf{1}]/[\mathbf{2}] \quad (1)$$

$$K^{III} = [\mathbf{2}^+]/[\mathbf{1}^+] \quad (2)$$

displays a characteristic absorption band near 640 nm which is absent for **1**. The intensity of this band was utilised to determine K^{II} at 303 K after equilibration for 12 h. The equilibrium constant K^{cr} of the cross-reaction (3) was utilised for

$$\mathbf{2} + \mathbf{1}^+ \overset{K^{cr}}{\rightleftharpoons} \mathbf{1} + \mathbf{2}^+ \quad (3)$$

$$K^{cr} = K^{II}K^{III} = \exp[F/RT(E^\circ_T(cis) - E^\circ_T(trans))] \quad (4)$$

determination of K^{III} from K^{II}, $E_{\frac{1}{2}}(cis)$ and $E_{\frac{1}{2}}(trans)$. Values of K^{II}, K^{III} and K^{cr} are listed in Table 5. For the bivalent complex the equilibrium concentration is more than 85% *cis* and for the trivalent complex it is virtually pure *trans*.

Origin of Isomer Preference: Comparisons.—The origin of isomer preference has been discussed in terms of structural parameters in our previous communication.[7] For completeness the main findings will be briefly stated here. In the case of osmium(II) the thermodynamically stable isomer is *cis*, **1**. This preference is due to stronger $5d_\pi$–$3d_\pi$ Os–P back bonding in **1** compared to **2**. The interphosphine *cis* interaction [13] reduces the stability of **1** but not sufficiently to offset the back-bonding advantage. Back bonding stabilises the metal $5d_\pi$ orbitals which therefore lie lower in **1** compared to **2**. The reduction potential order $E_{\frac{1}{2}}(cis) > E_{\frac{1}{2}}(trans)$ is consistent with this since the redox electron is a $5d_\pi$ electron. For osmium(III) the stable isomer is *trans*, $\mathbf{2}^+$. This is so because here back bonding is of limited significance [1] and interphosphine interaction plays the decisive role. The Os–P distance decreases in the order $\mathbf{2}^+ > \mathbf{2} > \mathbf{1}$.[7]

With this work we conclude our studies on isomer preference in species of type $[M(S\text{–}S)_2L_2]^z$ where M = Ru or Os, S–S = dithio- or trithio-carbonate and L = PPh_3.[3,7] All the four systems qualitatively behave in the same manner and the origin of the isomer preference is evidently the same in all cases. Quantitatively there are differences particularly between osmium and ruthenium as expected. We illustrate this with the help of the trithiocarbonates, R = Et. The reduction potentials are higher for ruthenium, *e.g.* $E_{\frac{1}{2}}(cis)$ = 0.43 (Os) and 0.61 V (Ru) and $E_{\frac{1}{2}}(trans)$ = 0.15 (Os) and 0.29V (Ru). The isomerisation rates are much slower for osmium *e.g.* for *cis* ⟶ *trans*, 2.6×10^{-5} (303 K) for Os^{II} and 3.3×10^{-2} s^{-1} (278 K) for Ru^{II}.

Table 4 Rate constants and activation parameters in dichloromethane for $[Os(RSCS_2)_2(PPh_3)_2]$

	trans ⟶ *cis*				*cis*$^+$ ⟶ *trans*$^+$			
R	T/K	10^5k^{II}/s^{-1}	$\Delta H^‡$/kJ mol^{-1}	$\Delta S^‡$/J K^{-1} mol^{-1}	T/K	10^2k^{III}/s^{-1}	$\Delta H^‡$/kJ mol^{-1}	$\Delta S^‡$/J K^{-1} mol^{-1}
Et	303	2.6	99.9	−34.9	248	4.4	46.9	−81.4
	308	4.8			253	7.5		
	313	8.4			258	10.8		
Pr^i	303	1.2	99.1	−14.4	248	2.8	49.4	−75.6
	308	2.2			253	4.6		
	313	4.3			258	7.3		
$PhCH_2$	303	1.5	91.8	−36.4	248	3.2	46.9	−84.6
	308	3.0			253	5.3		
	313	4.9			258	7.9		

Table 5 Equilibrium constants in dichloromethane at 303 K

Compound	K^{II}	$10^{-4}K^{cr}$	$10^{-3}K^{III}$
$[Os(EtSCS_2)_2(PPh_3)_2]$	8.33	4.49	5.40
$[Os(Pr^iSCS_2)_2(PPh_3)_2]$	5.90	2.12	3.60
$[Os(PhCH_2SCS_2)_2(PPh_3)_2]$	5.10	9.74	19.10

For ruthenium, the equilibrium constants K^{II} and K^{III} could not be experimentally determined since in either case the reaction proceeds very far to the right. This is indirectly reflected in the K^{cr} ($= K^{II}K^{III}$) values: $\approx 10^4$ (Os) and 10^6 (Ru). In summary, compared to osmium, ruthenium isomerises faster and more completely. For this reason the osmium systems have provided a better opportunity to map the isomerisation and redox equilibria embodied in Scheme 1.

Experimental

Materials.—The starting complex $[Os(PPh_3)_3Br_2]$ was synthesised from $[NH_4]_2[OsBr_6]$[14] by a reported method.[15] The $K[S_2CSR]$ salts were made as described.[16] The preparation of tetraethylammonium perchlorate and the purification of dichloromethane for electrochemical/spectroscopic work were done as before.[8] All other chemicals and solvents were of reagent grade used without further purification.

Physical Measurements.—The UV/VIS/NIR spectra were recorded by using a Hitachi 330 spectrophotometer, infrared (4000–300 cm^{-1}) spectra on a Perkin-Elmer 783 spectrophotometer. Magnetic susceptibility was measured on a PAR 155 vibrating-sample magnetometer fitted with a Walker Scientific L75FBAL magnet. X-Band EPR spectra were recorded on a Varian E-109C spectrometer fitted with a quartz Dewar flask for measurements at 77 K (liquid nitrogen), and calibrated with respect to diphenylpicrylhydrazyl (dpph) ($g = 2.0037$). Electrochemical measurements were done by using a PAR model 370-4 electrochemistry system as described elsewhere.[3c] All experiments were performed under a dinitrogen atmosphere and reported potentials are uncorrected for the junction contribution. Haake model-F3K and model-D8G digital cryostats and circulators connected to appropriate jacketed cells were used for low-temperature measurements. Solution electrical conductivity was measured by using a Philips PR 9500 bridge. Microanalytical data (C, H and N) were obtained with the use of a Perkin-Elmer model 240C elemental analyser.

Preparation of Complexes.—Complexes were prepared by using general procedures, in yields of 90–95%. Details are given only for a representative example of each type.

cis-*Bis(benzyl trithiocarbonato*-S,S′*)bis(triphenylphosphine)osmium*(II), *cis*-$[Os(PhCH_2SCS_2)_2(PPh_3)_2]$. A suspension of $[Os(PPh_3)_3Br_2]$ (200 mg, 0.18 mmol) in ethanol (35 cm^3) was warmed and $K(S_2CSCH_2Ph)$ (100 mg, 0.42 mmol) added. The mixture was heated to reflux for 1 h. Upon cooling a yellow microcrystalline solid separated which was collected by filtration, washed thoroughly with water and ethanol, and dried *in vacuo* over P_4O_{10}. Yield 180 mg.

trans-*Bis(benzyl trithiocarbonato*-S,S′*)bis(triphenylphosphine)osmium*(III) *hexafluorophosphate*, *trans*-$[Os(PhCH_2SCS_2)_2(PPh_3)_2]PF_6$. To a solution of pure *cis*-$[Os(PhCH_2SCS_2)_2(PPh_3)_2]$ (100 mg, 0.09 mmol) in dichloromethane–acetonitrile (1:10, 30 cm^3) was added ammonium cerium(IV) sulphate (95 mg, 0.15 mmol) dissolved in water (25 cm^3). The mixture was stirred at room temperature for 1 h. The colour became bluish green. The reaction mixture was then filtered and the filtrate reduced to 10 cm^3 under low pressure. A saturated aqueous solution of NH_4PF_6 (10 cm^3) was added. The blue-green solid thus obtained was collected by filtration, washed with water, and dried *in vacuo* over P_4O_{10}. It was dissolved in the minimum volume of dichloromethane and subjected to chromatography on a silica gel (60–120 mesh, BDH) column (20 × 1 cm). On elution with benzene–acetonitrile (9:1) a deep bluish green band was removed very rapidly and collected. The required complex was obtained from the eluent in crystalline form by slow evaporation. Yield 105 mg.

trans-*Bis(benzyl trithiocarbonato*-S,S′*)bis(triphenylphosphine)osmium*(II), *trans*-$[Os(PhCH_2SCS_2)_2(PPh_3)_2]$. The complex *trans*-$[Os(PhCH_2SCS_2)_2(PPh_3)_2]PF_6$ (100 mg, 0.08 mmol) was dissolved in acetonitrile (20 cm^3) and stirred magnetically at 273 K under a stream of nitrogen. Hydrazine hydrate (35 mg, 0.7 mmol) in acetonitrile (5 cm^3) was added dropwise. The bluish green solution immediately changed to pale green, and a solid separated. Stirring was continued for 10 min. The pale green solid thus obtained was collected by filtration, washed with water and acetonitrile and dried *in vacuo* over P_4O_{10}. Yield 80 mg.

Acknowledgements

We thank the Department of Science and Technology and the Council of Scientific and Industrial Research, New Delhi, India, for financial support.

References

1 H. Taube, *Surv. Prog. Chem.*, 1973, **6**, 1; H. Taube, *Pure Appl. Chem.*, 1979, **51**, 901; M. Sekine, W. D. Harman and H. Taube, *Inorg. Chem.*, 1988, **27**, 3604.

2 P. Basu, S. Pal and A. Chakravorty, *J. Chem. Soc., Chem. Commun.*, 1989, 977; P. Basu, S. Bhanja Choudhury, S. Pal and A. Chakravorty, *Inorg. Chem.*, 1989, **28**, 2680; D. Ray and A. Chakravorty, *Inorg. Chem.*, 1988, **27**, 3292.

3 (*a*) N. Bag, G. K. Lahiri and A. Chakravorty, *J. Chem. Soc., Dalton Trans.*, 1990, 1557; (*b*) A. Pramanik, N. Bag, G. K. Lahiri and A. Chakravorty, *J. Chem. Soc., Dalton Trans.*, 1990, 3823; (*c*) A. Pramanik, N. Bag, D. Ray, G. K. Lahiri and A. Chakravorty, *Inorg. Chem.*, 1991, **30**, 410.

4 A. M. Bond, B. S. Grabaric and Z. Grabaric, *Inorg. Chem.*, 1978, **17**, 1013; A. M. Bond, S. W. Carr and R. Colton, *Inorg. Chem.*, 1984, **23**, 2343; A. M. Bond, T. W. Hambley, D. R. Mann and M. R. Snow, *Inorg. Chem.*, 1987, **26**, 2257 and refs. therein.

5 R. D. Rieke, H. Kojima and K. Ofele, *J. Am. Chem. Soc.*, 1976, **98**, 6735; C. M. Elson, *Inorg. Chem.*, 1976, **15**, 469; A. Vallat, M. Person, L. Roullier and E. Laviron, *Inorg. Chem.*, 1987, **26**, 332; M. M. Bernardo, P. V. Robandt, R. R. Schroeder and D. B. Rorabacher, *J. Am. Chem. Soc.*, 1989, **111**, 1224.
6 B. E. Bursten, *J. Am. Chem. Soc.*, 1982, **104**, 1299; D. M. P. Mingos, *J. Organomet. Chem.*, 1979, **179**, C29.
7 A. Pramanik, N. Bag, D. Ray, G. K. Lahiri and A. Chakravorty, *J. Chem. Soc., Chem. Commun.*, 1991, 139.
8 G. K. Lahiri, S. Bhattacharya, B. K. Ghosh and A. Chakravorty, *Inorg. Chem.*, 1987, **26**, 4324; G. K. Lahiri, S. Bhattacharya, M. Mukherjee, A. K. Mukherjee and A. Chakravorty, *Inorg. Chem.*, 1987, **26**, 3359.
9 B. Bleaney and M. C. M. O'Brien, *Proc. Phys. Soc. London, Sect. B*, 1956, **69**, 1216; J. S. Griffith, *The Theory of Transitional Metal Ions*, Cambridge University Press, London, 1961, p. 364.
10 S. Sakaki, N. Hagiwara, Y. Yanase and A. Ohyoshi, *J. Phys. Chem.*, 1978, **82**, 1917; A. Hudson and M. J. Kennedy, *J. Chem. Soc. A*, 1969, 1116.
11 R. S. Nicholson and I. Shain, *Anal. Chem.*, 1964, **36**, 706.
12 N. Serpone and D. G. Bickley, *Prog. Inorg. Chem.*, 1972, **17**, 391 and refs. therein.
13 C. A. Tolman, *Chem. Rev.*, 1977, **77**, 313; H. C. Clark and M. J. Hampden-Smith, *Coord. Chem. Rev.*, 1987, **79**, 229; J. Powell, *J. Chem. Soc., Chem. Commun.*, 1989, 200.
14 F. P. Dwyer and J. W. Hogarth, *Inorg. Synth.*, 1957, **5**, 204.
15 P. R. Hoffman and K. G. Caulton, *J. Am. Chem. Soc.*, 1975, **97**, 4221.
16 J. Hyde, K. Venkatasubramanian and J. Zubieta, *Inorg. Chem.*, 1978, **17**, 414.

Received 21*st May* 1991; *Paper* 1/02385C